Microbial battery for efficient energy recovery

Xing Xie[a,b], Meng Ye[a], Po-Chun Hsu[b], Nian Liu[c], Craig S. Criddle[a,1], and Yi Cui[b,d,1]

Departments of [a]Civil and Environmental Engineering, [b]Materials Science and Engineering, and [c]Chemistry, Stanford University, Stanford, CA 94305; and [d]Stanford Institute for Materials and Energy Sciences, SLAC National Accelerator Laboratory, Menlo Park, CA 94025

Edited by Harry B. Gray, California Institute of Technology, Pasadena, CA, and approved August 9, 2013 (received for review April 18, 2013)

By harnessing the oxidative power of microorganisms, energy can be recovered from reservoirs of less-concentrated organic matter, such as marine sediment, wastewater, and waste biomass. Left unmanaged, these reservoirs can become eutrophic dead zones and sites of greenhouse gas generation. Here, we introduce a unique means of energy recovery from these reservoirs—a microbial battery (MB) consisting of an anode colonized by microorganisms and a reoxidizable solid-state cathode. The MB has a single-chamber configuration and does not contain ion-exchange membranes. Bench-scale MB prototypes were constructed from commercially available materials using glucose or domestic wastewater as electron donor and silver oxide as a coupled solid-state oxidant electrode. The MB achieved an efficiency of electrical energy conversion of 49% based on the combustion enthalpy of the organic matter consumed or 44% based on the organic matter added. Electrochemical reoxidation of the solid-state electrode decreased net efficiency to about 30%. This net efficiency of energy recovery (unoptimized) is comparable to methane fermentation with combined heat and power.

bioelectrochemical system | microbial fuel cells | exoelectrogens | renewable energy

Current global energy demand is ~5.3×10^{20} J/y (1). Most of this demand (>80%) is met by extraction and oxidation of the fossil carbon present in concentrated organic reservoirs as oil (32%), coal (27%), and natural gas (21%) (1). About 31% (1.7×10^{20} J/y) is used to produce 7.7×10^{19} J/y of electrical energy with an energy conversion efficiency of ~46% (1). The proven untapped reserves of oil, coal, and natural gas are 9.1×10^{22} J (2). Without carbon sequestration, these supplies would result in significant greenhouse gas emissions (1, 3). Identification of supplies that avoid such releases is a pressing challenge (4). One promising option is the use of less-concentrated reservoirs of organic matter. An untapped resource is the organic matter in marine sediment, estimated to contain 5.2×10^{22} J of stored chemical energy if oxidized with oxygen (5). Other reservoirs of less-concentrated organic matter are also as yet untapped—in part because they are often viewed as waste, and in part because the technology needed to recover energy from less-concentrated reservoirs is inefficient. If not oxidized, these organics can deplete the oxygen reserves of aquatic ecosystems and stimulate release of methane to the atmosphere. An example is domestic wastewater, a threat to aerobic aquatic ecosystems. The organic matter in domestic wastewater is theoretically sufficient to generate ~7.4×10^{18} J/y: three to four times more energy than is needed to treat the wastewater (6). However, 3% of the electrical load of developed countries is currently required to treat wastewater (7). Another waste example is the biomass produced through photosynthesis, most of which is not used for human needs. Globally, 4.5×10^{21} J/y are stored in biomass generated by photosynthesis (8). About 1% (5.0×10^{19} J/y) is harvested for human energy needs (9). The remaining biomass can undergo uncontrolled anaerobic biodegradation, with ensuing greenhouse gas emissions.

Effective energy extraction from less-concentrated organic reservoirs can potentially be achieved with microbial biotechnology. Self-assembled microbial communities have optimized energy extraction systems that allow efficient in situ oxidation of organic matter and other electron donors in diverse environments (4). Because these systems evolved under strong competitive pressures to meet microbial needs for energy (10), hijacking them for human purposes requires understanding of factors that influence microbial competition for energy. The most important factor is the nature of the available oxidants. In reservoirs rich in electron donors, the strongest oxidant (O_2 in aerobic systems) is used first, followed by use of progressively weaker oxidants [NO_3^- > Mn (IV) minerals > Fe(III) minerals > SO_4^{2-} > CO_2] (10). Carbon dioxide, the least powerful oxidant, is used last and is often the sole remaining oxidant in electron donor-rich anaerobic environments. A significant fraction of the electrons removed (~90%) is transferred to methane which can concentrate in the gas phase (11). The high efficiency of electron transfer to methane and the ease of methane recovery from water make methane fermentation a useful benchmark for energy recovery via microbial biotechnology. However, use of methane fermentation for energy generation has limitations: efficient digestion of biomass requires hydrolysis and fermentation at warm temperatures (>20 °C) (6, 11); inefficient capture of methane and losses during transport lead to energy losses, greenhouse gas emissions, and explosion hazards; and the collected biogas often requires clean-up to remove contaminants (hydrogen sulfide and siloxanes), limiting applications to large-scale digesters (12).

Microbial fuel cells (MFCs) offer an option for direct electricity generation from electron donors oxidized by microorganisms (13) and have been used to recover electricity from domestic wastewater and marine sediment (6, 14–16). Like chemical fuel cells, oxidation occurs at an anode, and electrons pass through an external circuit to a cathode where O_2 is reduced. At the anode, however, chemical catalysts are replaced by exoelectrogens—microorganisms that oxidize the electron donors and transfer the electrons to an electrode (17). For MFCs, energy recovery is limited by a voltage loss when O_2 is reduced at the cathode. This loss is exacerbated by MFC operating conditions—atmospheric pressure, ambient temperature, and an aqueous

Significance

This work introduces a microbial battery for recovery of energy from reservoirs of organic matter, such as wastewater. Microorganisms at an anode oxidize dissolved organic substances, releasing electrons to an external circuit, where power can be extracted. The electrons then enter a solid-state electrode that remains solid as electrons accumulate within it. The solid-state electrode is periodically removed from the battery, oxidized, and reinstalled for sustained power production. Molecular oxygen is not introduced into the battery, and ion-exchange membranes are avoided, enabling high efficiencies of energy recovery.

Author contributions: X.X., C.S.C., and Y.C. designed research; X.X., M.Y., P.-C.H., and N.L. performed research; X.X., M.Y., C.S.C., and Y.C. analyzed data; and X.X., M.Y., P.-C.H., N.L., C.S.C., and Y.C. wrote the paper.

The authors declare no conflict of interest.

This article is a PNAS Direct Submission.

[1]To whom correspondence may be addressed. E-mail: yicui@stanford.edu or ccriddle@stanford.edu.

This article contains supporting information online at www.pnas.org/lookup/suppl/doi:10.1073/pnas.1307327110/-/DCSupplemental.

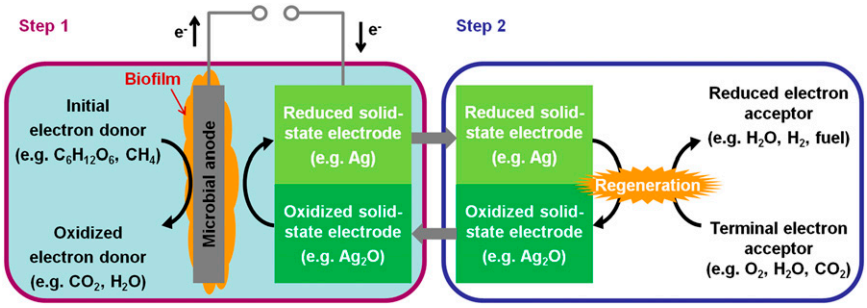

Fig. 1. Schematic of two-step energy generation process using microbial batteries (MBs). In step 1, electron donors are oxidized by microorganisms, releasing electrons to an intermediate solid-state electrode; in step 2, the solid-state electrode is regenerated by supplying a terminal electron acceptor. The key components are a microbial anode and a solid-state oxidant cathode. Organics are oxidized at the anode by the enzymatic activity of exoelectrogens. At the cathode, a solid-state oxidant is reduced.

electrolyte at near-neutral pH. Diffusion of dissolved O_2 into the anode compartment is also a problem, allowing formation of aerobic biomass and oxidation of organic matter without energy production. Finally, methane production is sometimes reported in the anode compartment (18). This represents yet another energy loss and signals that methanogens are outcompeting exoelectrogens for the available electrons. Building on previous MFC studies, this work introduces a previously undescribed microbial electrochemical device for energy recovery where the key difference is the use of a solid-state cathode to replace the oxygen gas cathode of a MFC. Operation of the anode is like that of a MFC anode, but operation of the cathode is like that of a rechargeable battery. We therefore refer to this device as a microbial battery (MB).

Results and Discussion

Sustained operation of the MB system requires two steps. In step 1, microorganisms at the anode oxidize electron donors (e.g., carbohydrates and methane), releasing electrons that pass through an external circuit to a cathode comprising (or containing) a solid-state oxidant, such as silver oxide (Fig. 1, step 1). The cathode material becomes reduced. In the case of a silver-oxide electrode, silver metal is produced. Step 1 is an energy extraction process like that of the discharge process in batteries. In step 2, the cathode is removed and oxidized by exposure to a terminal electron acceptor, such as oxygen, water, or carbon dioxide, under conditions favorable for its oxidation (Fig. 1, step 2). The oxidized electrode is then reinstalled—a step that differs only slightly from the normal process used to recharge batteries—and the process is repeated. The major drawbacks of MFCs—voltage losses at oxygen cathodes and diffusion of oxygen into the anode compartment—are avoided by single-chamber operation without the introduction of oxygen.

A design challenge for the MB is identification of a stable solid-state electrode with a suitable electrochemical potential.

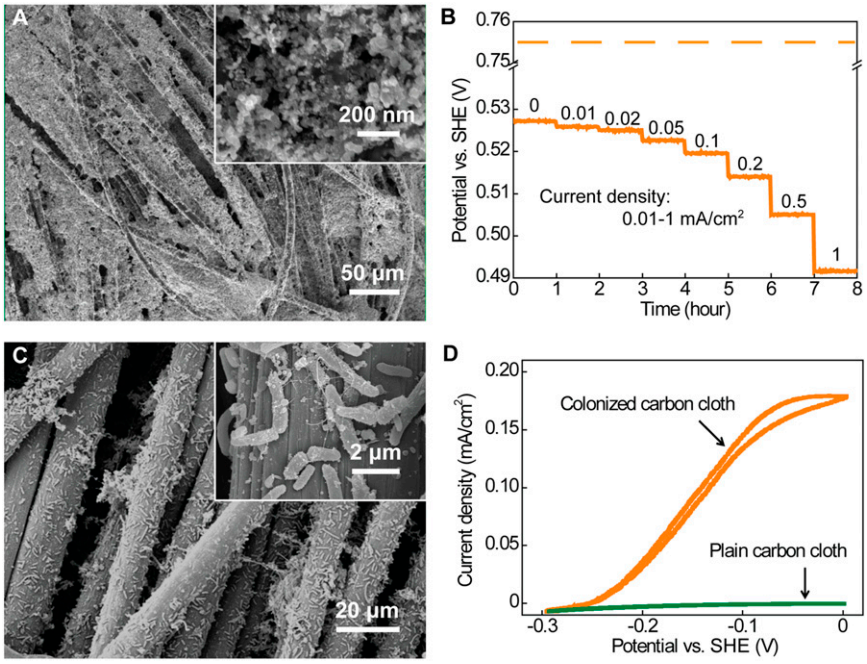

Fig. 2. Carbon cloth-supported silver-oxide cathode (*A* and *B*) and carbon cloth microbial anode (*C* and *D*). (*A*) Scanning electron microscope (SEM) images of a silver-oxide electrode. The particles are less than 50 nm. (*B*) Reduction potential of a silver-oxide electrode in a phosphate buffer solution (PBS, 200 mM, pH 7) at current densities ranging from 0.01 to 1 mA/cm^2. Current density values are labeled above the potential curve. The dashed line indicates the standard reduction potential. (*C*) SEM images of a colonized carbon cloth electrode. Zoom-in image (*Inset*) shows a cluster of exoelectrogens connected by microbial nanowires. (*D*) Cyclic voltammograms (CVs) of a colonized carbon cloth electrode and a plain carbon cloth electrode in a glucose electrolyte (~1 g/L). Scan rate, 1 mV/s.

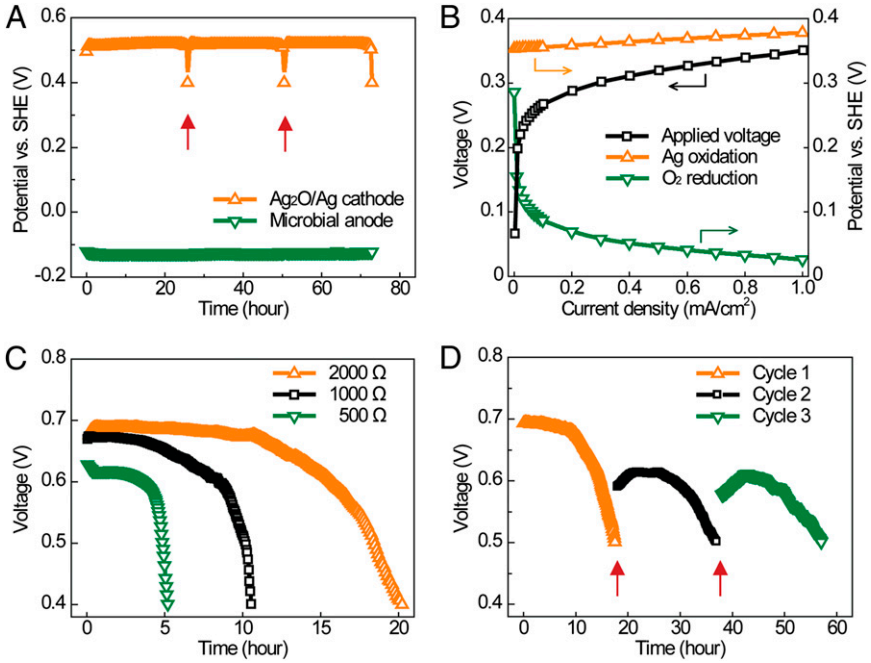

Fig. 3. Performance of glucose-fed MBs and regeneration of the solid-state Ag_2O/Ag electrode. (*A*) Potentials of the microbial anode and the Ag_2O/Ag electrode during oxidation of a glucose solution (~1 g/L) at a fixed current density of 0.1 mA/cm^2. The red arrows indicate regeneration of the Ag_2O/Ag electrode. (*B*) Polarization curves show the applied voltage and potentials of both electrodes during regeneration of the Ag_2O/Ag electrode with O_2 reduction catalyzed by a commercially available carbon cloth supported platinum (Pt) electrode. The electrolyte was a sodium hydroxide (NaOH, 1 M, pH 14) solution bubbled with air (~100 mL/min). After changing the current density, potentials were recorded until equilibrium was reached (at least 10 min). (*C* and *D*) Voltage profiles of plate-shaped MBs with different external loadings (*C*) and in three consecutive cycles with a 2,000 Ω loading. The MBs were equipped with precolonized carbon cloth anodes and silver-oxide cathodes. The feeding was a glucose solution (~1 g/L). The red arrows in *D* indicate the replacement of fresh glucose feeding and the regeneration of the Ag_2O/Ag electrode.

One candidate couple is silver oxide/silver (Ag_2O/Ag), a couple that has been used for decades in batteries (19). This couple offers several advantages: (*i*) both silver and silver oxide remain in the solid state in water and are stable under conditions favorable for microbial growth, i.e., ambient pressure and temperature and near-neutral pH; (*ii*) the standard reduction potential at pH 7 is 0.76 V vs. standard hydrogen electrode (SHE)—a value that is higher than the value for other electron acceptors commonly present in anaerobic environments (such as SO_4^{2-} and CO_2), but lower than oxygen evolution (0.82 V vs. SHE at pH 7); (*iii*) the potential difference between the anode and the silver oxide electrode is large enough to support energy extraction for human needs and to also sustain exoelectrogen growth and competition for electron donors (11, 17); (*iv*) hydroxyl alkalinity generated by reduction of silver oxide to silver at the cathode neutralizes acidity produced at the anode; and (*v*) silver has well-documented antimicrobial properties, preventing growth of microorganisms on the silver-oxide electrode and enabling operation within a single chamber without an ion-exchange membrane.

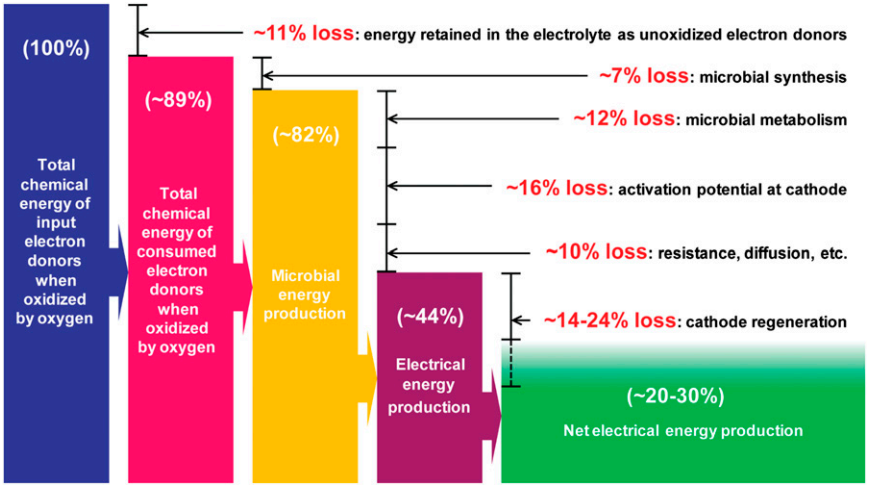

Fig. 4. MB energy recovery with a 2,000 Ω loading and a Ag_2O/Ag solid-state electrode with coupled electrochemical regeneration of the Ag_2O/Ag electrode. The heights of the boxes indicate the energy percentages.

Electrode samples were prepared by embedding silver nanoparticles on a carbon cloth substrate followed by electrochemical oxidation (*SI Appendix*, Fig. S1). X-ray diffraction (XRD) verified the formation of silver oxide (*SI Appendix*, Fig. S2). Scanning electron microscope (SEM) images of the electrode surface are shown in Fig. 2*A*. The silver-oxide electrodes were tested in a phosphate buffer solution (PBS, 200 mM, pH 7) to simulate operational conditions in MBs. The reduction potential under different current densities was recorded (Fig. 2*B*). Electrode potentials were constant during reduction, indicating that solid-phase reduction of silver oxide to silver was stable. With reducing currents that varied from 0.01 to 1 mA/cm^2 (a typical operating current density range for microbial anodes), the reduction potentials of the electrodes remained stable at 0.53–0.49 V vs. SHE (Fig. 2*B* and *SI Appendix*, Fig. S3). These values were much higher than those of oxygen reduction (from 0.43 to −0.07 V vs. SHE) catalyzed by a commercially available platinum (Pt) electrode (Pt nanoparticles on a carbon cloth substrate) under the same conditions (*SI Appendix*, Fig. S3). Higher voltage outputs are attributed to lower overpotential losses (0.23–0.27 V for Ag_2O vs. 0.39–0.89 V for O_2), and the superior electrochemical properties of the Ag_2O/Ag couple. When the same Ag_2O/Ag electrode was operated in a sodium hydroxide electrolyte (NaOH, 1 M, pH 14), a typical condition in Ag_2O/Ag batteries, the overpotential loss was less than 0.05 V at a current density of 1 mA/cm^2 (*SI Appendix*, Fig. S4). The greater losses observed in the PBS electrolyte were probably due to surface changes in the Ag_2O/Ag electrode at neutral pH or local increase in pH near the Ag_2O/Ag electrode surface during reduction.

The anode materials for MBs can be carbon cloth (20), graphite brush (21), or carbon nanotube/graphene-coated macroporous substrate, such as sponge (22, 23). Fig. 2*C* shows SEM images of a commercially available carbon cloth electrode colonized by exoelectrogens. The exoelectrogens remove electrons from electron donors in the electrolyte and transfer the electrons to the electrode by direct surface contact, diffusion of electron shuttles, and/or conduction through microbial nanowires (17, 24, 25). Electrochemical impedance spectroscopy (*SI Appendix*, Fig. S5) and cyclic voltammetry (Fig. 2*D*) established that exoelectrogens were actively oxidizing organics: In electrolyte amended with glucose (~1 g/L, an electron-equivalent concentration similar to that of typical domestic wastewater), a strong signal for electron transfer was only seen with carbon cloth colonized by microorganisms (*SI Appendix*, Fig. S5), and a positive current peak resulted from the oxidation of glucose (Fig. 2*D*).

Single-chamber MBs were built by placing the precolonized microbial anodes and silver-oxide cathodes into a bottle containing 100 mL glucose electrolyte (~1 g/L). The potentials of the microbial anode and the Ag_2O/Ag electrode were recorded for a fixed current density of 0.1 mA/cm^2. As shown in Fig. 3*A*, the anode potential was stable at −0.12 V vs. SHE. This indicates that anode microbial activity was not affected by colocation of the Ag_2O/Ag electrode in the same chamber. Because the volume of the system was large and the current relatively small, the decrease in glucose levels was not large enough to change the anode potential. The operating potential of the Ag_2O/Ag electrode was about 0.52 V. The potential dropped quickly when the Ag_2O/Ag electrode reached its capacity for storage of electrons, and most of the silver oxide was reduced to silver. At this point, the Ag_2O/Ag electrode requires removal and regeneration with a terminal electron acceptor, such as oxygen (Fig. 1, step 2).

Reoxidation of silver by oxygen to silver oxide is thermodynamically favorable ($\Delta G = -22.6$ kJ/mol at 25 °C and 1 atm O_2) and is therefore expected to occur spontaneously (26). A thin silver-oxide layer is in fact observed when a clean silver surface is exposed to oxygen at normal pressures (27, 28). Complete oxidation occurs at 300 °C and 2 MPa O_2 (29). Simply bubbling oxygen through an aqueous solution of silver nanoparticles results in partial oxidation (30). Three different regeneration methods were investigated: direct exposure to air at room temperature (~20 °C), exposure to air at 90 °C, and immersion in aerated water bubbled with air. In all cases, the open circuit potential of the Ag_2O/Ag electrode returned to about 0.48 V vs. SHE after regeneration, but the operating potential dropped significantly when a reducing current was applied (*SI Appendix*, Fig. S6*A*). The oxidation capacity—defined as the amount of charge delivered to the cathode before the operating potential of the Ag_2O/Ag electrode fell to values less than 0.3 V vs. SHE—increased with the regeneration time (*SI Appendix*, Fig. S6*B*). After a 24-h regeneration period, the oxidation capacity could last for a few minutes when the reducing current was 0.1 mA/cm^2 (*SI Appendix*, Fig. S6*A*). Direct oxidation through such means could avoid use of noble metal catalysts for electrochemical reduction of O_2. Electrochemical reoxidation is also an option for regeneration. Because this step occurs outside the MB, temperature, pressure, and electrolyte composition can be optimized. As proof-of-concept, we used a sodium hydroxide solution (NaOH, 1 M, pH 14) as the electrolyte and a commercially available Pt electrode for oxygen reduction. As shown by the polarization curves in Fig. 3*B*, a voltage of 0.20–0.35 V was needed at a regeneration current of 0.01–1 mA/cm^2. After regeneration, the Ag_2O/Ag electrode was reinstalled in the MB with resumption of energy recovery (Fig. 3*A*). Because the Ag_2O/Ag redox couple is reversible, the charge-discharge of Ag_2O/Ag electrode in a NaOH electrolyte had a coulombic efficiency >97% over 200 cycles. A 20% drop in charge storage capacity occurred over the first 30 cycles—probably due to some loss of Ag_2O/Ag, but ~70% of the capacity remained after 200 cycles (*SI Appendix*, Fig. S7).

Plate-shaped MBs with compact design (3 × 3 × 0.3 cm^3) were constructed with precolonized microbial anodes (3 × 3 cm^2) and silver-oxide cathodes (3 × 3 cm^2) to estimate the efficiencies of MBs (*SI Appendix*, Fig. S8). The chamber was filled with 2 mL of glucose solution with an initial chemical oxygen demand (COD) of 1,170 mg/L. In this case, the oxidation capacity of the Ag_2O/Ag electrode was sufficient to maintain a stable operating potential for one cycle, whereas potential of the microbial anode changed as glucose concentration became limiting. Output voltage of the cell decreased. The open circuit voltage was 0.78 V. With a 2,000-Ω external loading, the maximum output voltage was 0.69 V (Fig. 3*C*). When the voltage dropped to 0.4 V, solution COD decreased to 130 mg/L, a removal efficiency of 89%. The total charge, calculated by integrating the generated current over time, established that ~92% of the organics removed were

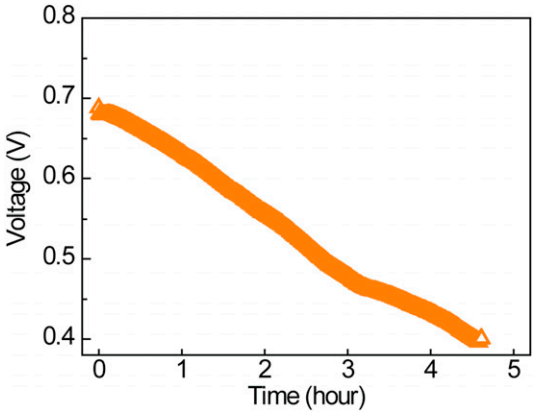

Fig. 5. Voltage profile of a plate-shaped MB oxidizing municipal wastewater organic matter with a 2,000 Ω loading. The MBs were equipped with precolonized carbon cloth anodes and silver-oxide cathodes. The feed was domestic wastewater with an initial COD of 390 ± 38 mg/L.

oxidized and contributed to current generation. No microbial growth was observed on the Ag_2O/Ag cathode. Operation at two other loadings (1,000 Ω and 500 Ω) was also investigated (Fig. 3*C*) with similar results. COD removal efficiencies were 91 and 92% for 1,000 Ω and 500 Ω loadings, respectively, and, in both cases, coulombic efficiency was 91%. Fig. 3*D* shows the voltage profiles of plate-shaped MBs in three consecutive cycles with a 2,000-Ω loading. A higher voltage cutoff of 0.5 V was applied to maintain microbial activity over multiple cycles. The performance of the later two cycles was similar. The maximum output voltages (~0.62 V) were not as high as the first cycle, probably because there was insufficient time for recovery of microbial activity before glucose concentration again became limiting. COD removal efficiencies were 85 (cycle 1), 84 (cycle 2), and 82% (cycle 3), and coulombic efficiencies were 91–92% in all cases.

Fig. 4 summarizes the energy flow of the MB with a 2,000-Ω load (Fig. 3*C*) followed by electrochemical regeneration of the solid-state (Ag_2O/Ag) electrode (*SI Appendix*, for calculation details, and Figs. S9 and S10). For this analysis, we consider all of the added glucose and assume that the total chemical energy is the combustion energy (2.8×10^3 kJ/mol for glucose) (26). This assumption enables comparison with energy conversion by methane fermentation with combined heat and power (CHP). The energy balance is as follows: about 11% of the energy in the added glucose is retained in the electrolyte as residual electron donors; of the 89% removed, ~7% is used for biomass synthesis, leaving ~82% for microbial energy production; ~12% is used for microbial metabolism; overpotential at the solid-state electrode resulted in another 16% energy loss; and 10% energy loss resulted from losses due to internal resistance and diffusion limitations. The gross efficiency of electrical energy production was ~44%. This number increases to ~49% if the energy recovered is divided by the energy of the organic matter consumed. The energy required for electrochemical reoxidation ranged from ~14–24%, depending upon the current density (0.01–1 mA/cm^2) applied. This step involves a tradeoff: reoxidization at higher current densities consumes more energy but is more rapid, so less electrode material is required for continuous electricity generation. The net energy conversion efficiency for energy production and electrode reoxidation was ~20–30% based on the organic matter added and ~21–33% based on the organic matter consumed. These values are comparable to methane fermentation with CHP (7).

The MB offers an alternative for energy recovery from soluble electron donors. Compared with methane production with CHP, it is likely to have fewer safety concerns and reduced environmental impact because methane production is avoided. The single-chamber design without ion-exchange membranes should be adaptable to different scales of operation. An obvious application is removal of biodegradable organics from domestic and industrial wastewaters. The same plate-shaped MB was tested with real domestic wastewater collected from a sewer at Escondido Village at Stanford University. Fig. 5 illustrates the voltage profile for oxidation of this wastewater-fed MB with a 2,000-Ω external loading. The voltage profile decreased gradually from 0.69 to 0.4 V during operation. This differed from the voltage profile of the glucose-fed MB, where a stable voltage plateau was followed by a decrease as glucose levels became limiting. This difference was likely due to differences in the biodegradability of municipal wastewater organics, with initial oxidation of readily biodegradable substances followed by oxidation of less-biodegradable substances. The COD removal efficiency was 53% from 390 to 170 mg/L, and the coulombic efficiency was 84%. The efficiency of electrical energy conversion was 38% based on the combustion enthalpy of COD removed or 22% based on total COD in the wastewater. The results demonstrate that the MB concept can be generalized for treatment of complex organic mixtures. For larger-scale applications, however, the high capital cost of the silver-based electrode would be prohibitive. More cost-effective materials are needed for fabrication of rechargeable solid-state electrodes.

Materials and Methods

Silver-oxide electrodes were prepared using a slurry-coating process followed by electrochemical oxidation. Silver nanoparticles (20 nm, SkySpring Nanomaterials, Inc., 85% wt) were mixed with conductive carbon black (Super-P, TIMCAL, 8% wt) and PVDF (Sigma-Aldrich, 7% wt) in NMP (Sigma-Aldrich). The mixture was stirred overnight and successively coated onto a carbon cloth (Fuel Cell Earth, LLC). The electrodes were dried in vacuum, resulting in a mass loading of ~20 mg/cm^2. The silver electrode was then oxidized electrochemically in a sodium hydroxide solution (NaOH, 1 M, pH 14) at a current density of 1 mA/cm^2. The process was stopped after the potential increased to 0.3 V vs. Ag/AgCl to avoid formation of silver peroxide (AgO). A carbon cloth-supported platinum (Pt) electrode (Pt loading 0.5 mg/cm^2, Fuel Cell Earth, LLC) was used for oxygen reduction. Carbon cloth microbial anodes were used. These anodes were colonized in traditional H-shaped MFCs for more than 1 mo until a stable current was obtained (22). Titanium wires were used to connect the electrodes to the external circuits.

Plate-shaped MBs were manufactured at the Varian Physics Machine Shop at Stanford. Two pieces of Plexiglas, with a groove of $3 \times 3 \times 0.15$ cm on each piece, were screwed together to form a chamber of $3 \times 3 \times 0.3$ cm. A pre-colonized carbon cloth microbial anode (3×3 cm) and a carbon cloth-supported silver-oxide cathode (3×3 cm) were installed on each side with a separation distance of about 0.2 cm. Different resistors (500–2,000 Ω) were applied as external loading, and the output voltages were recorded. The MBs were first filled with a phosphate buffer (PBS, 200 mM, pH 7). Oxidation of residual organic matter was accompanied by a decline in output voltage to 0.4 V. The electrolyte volume (2 mL) was replaced with fresh PBS buffer containing ~1 g/L glucose, and the current generation cycle was repeated. After the output voltage returned to 0.4 V, operation was stopped and the electrolyte analyzed.

Electrochemical characterization was achieved with a three-electrode setup using a BioLogic VMP3 potentiostat-galvanostat equipped with an electrochemical impedance spectroscopy (EIS) board. A double-junction Ag|AgCl|KCl (3.5 M) reference electrode (RE) was used for the measurement, with a Pt counter electrode (CE) used as necessary. EIS was conducted at the open circuit voltage (OCV) in the frequency range of 10^5–0.1 Hz with a 10 mV peak-to-peak sinusoidal potential perturbation. Cyclic voltammetry tests were performed on the microbial anodes over the potential range, −0.5 to −0.2 V vs. RE at a sweep rate of 1 mV/s. Polarization curves were obtained by changing the current density from 0.01 to 1 mA/cm^2 and monitoring potential until equilibrium was observed (at least 10 min). Oxygen reduction measurements were performed while the electrolyte was bubbled with air (~100 mL/min). XRD measurements were carried out with a PANalytical X'Pert (Ni-filtered Cu Kα radiation), and scanning electron microscope (SEM) images were taken by FEI Nova NanoSEM. For SEM, the anode sample was pretreated with a fixing and critical point-drying process (22). The COD of the electrolyte was determined using a HACH COD analysis kit (HACH, Co.).

ACKNOWLEDGMENTS. X.X. acknowledges the support from the Stanford Interdisciplinary Graduate Fellowship.

1. International Energy Agency (2012) *Key World Energy Statistics* (Int Energy Agency, Paris).
2. British Petroleum (2011) *Statistical Review of World Energy* (Brit Pet, London).
3. Intergovernmental Panel on Climate Change (2001) *Climate change 2001: The scientific basis* (Intergov Panel Clim Change, Cambridge United Kingdom).
4. Tiedje J, Donohue T (2008) Microbes in the energy grid. *Science* 320(5879):985.
5. Yen TF ed (1977) *Chemistry of Marine Sediments* (Ann Arbor Sci, Ann Arbor, MI).
6. Logan BE, Rabaey K (2012) Conversion of wastes into bioelectricity and chemicals by using microbial electrochemical technologies. *Science* 337(6095):686–690.
7. McCarty PL, Bae J, Kim J (2011) Domestic wastewater treatment as a net energy producer—can this be achieved? *Environ Sci Technol* 45(17):7100–7106.
8. Sims REH ed (2003) *Bioenergy Options for a Cleaner Environment* (Elsevier, Amsterdam).
9. Ladanai S, Vinterbäck J (2009) *Global Potential of Sustainable Biomass for Energy* (Swed Univ Agric Sci, Uppsala).
10. Madigan MT, Martinko JM (2006) *Brock Biology of Microorganisms* (Pearson Ed, Upper Saddle River, NJ).
11. Rittmann BE, McCarty PL (2001) *Environmental Biotechnology: Principles and Applications* (McGraw-Hill, New York).

12. Environmental Protection Agency (2007) *Opportunities for and Benefits of Combined Heat and Power at Wastewater Treatment Facilities* (Environ Prot Agency, Washington, DC).
13. Chaudhuri SK, Lovley DR (2003) Electricity generation by direct oxidation of glucose in mediatorless microbial fuel cells. *Nat Biotechnol* 21(10):1229–1232.
14. Tender LM, et al. (2002) Harnessing microbially generated power on the seafloor. *Nat Biotechnol* 20(8):821–825.
15. Bond DR, Holmes DE, Tender LM, Lovley DR (2002) Electrode-reducing microorganisms that harvest energy from marine sediments. *Science* 295(5554):483–485.
16. Liu H, Ramnarayanan R, Logan BE (2004) Production of electricity during wastewater treatment using a single chamber microbial fuel cell. *Environ Sci Technol* 38(7):2281–2285.
17. Logan BE (2009) Exoelectrogenic bacteria that power microbial fuel cells. *Nat Rev Microbiol* 7(5):375–381.
18. Rabaey K, Verstraete W (2005) Microbial fuel cells: Novel biotechnology for energy generation. *Trends Biotechnol* 23(6):291–298.
19. Rao MLB, Anantharaman PN, Mathur PB (1963) Production of positive plates for silver oxide-zinc batteries. *Ind Eng Chem Prod Res Dev* 2(2):155–157.
20. Cheng S, Liu H, Logan BE (2006) Increased power generation in a continuous flow MFC with advective flow through the porous anode and reduced electrode spacing. *Environ Sci Technol* 40(7):2426–2432.
21. Logan B, Cheng S, Watson V, Estadt G (2007) Graphite fiber brush anodes for increased power production in air-cathode microbial fuel cells. *Environ Sci Technol* 41(9):3341–3346.
22. Xie X, et al. (2012) Carbon nanotube-coated macroporous sponge for microbial fuel cell electrodes. *Energy Environ. Sci.* 5(1):5265–5270.
23. Xie X, et al. (2012) Graphene-sponge as high-performance low-cost anodes for microbial fuel cells. *Energy Environ. Sci.* 5(5):6862–6866.
24. Reguera G, et al. (2005) Extracellular electron transfer via microbial nanowires. *Nature* 435(7045):1098–1101.
25. Gorby YA, et al. (2006) Electrically conductive bacterial nanowires produced by *Shewanella oneidensis* strain MR-1 and other microorganisms. *Proc Natl Acad Sci USA* 103(30):11358–11363.
26. Haynes WM ed (2013) *Handbook of Chemistry and Physics* (CRC Press, Boca Raton, FL), 94th Ed.
27. de Rooij A (1989) The oxidation of silver by atomic oxygen. *Eur. Space Agency J* 13(4): 363–382.
28. Rehren C, Muhler M, Bao X, Schlogl R, Ertl G (1991) The interaction of silver with oxygen: an investigation with thermal desorption and photoelectron spectroscopy. *Z Phys Chem* 174(1):11–52.
29. Lavrenko VA, Malyshevskaya AI, Kuznetsova LI, Litvinenko VF, Pavlikov VN (2006) Features of high-temperature oxidation in air of silver and alloy Ag-Cu, and adsorption of oxygen on silver. *Powder Metall Met Ceram* 45(9-10):476–480.
30. Lok C-N, et al. (2007) Silver nanoparticles: Partial oxidation and antibacterial activities. *J Biol Inorg Chem* 12(4):527–534.

Supplementary Discussion

The following sections provide experimental details and MB recovery calculations for energy with a 2000 Ω loading equipped with a Ag_2O/Ag solid-state electrode, including reduction of the electrode by its electrochemical re-oxidation.

Total chemical energy input.

The initial chemical oxygen demand (COD) of the feed solution was 1170 mg/L. One mole of glucose has an oxygen demand of 192 g, so the initial glucose concentration was:

$$\frac{1170 \text{ mg COD/L}}{1000 \text{ mg/g} \times 192 \text{ g COD/mol}} = 6.1\times10^{-3} \text{ mol/L}$$

The effective volume of the plate-shaped MB is 2 mL, and the combustion enthalpy of glucose is 2.8×10^6 J/mol. This gives a total chemical energy input of:

$$\frac{6.1\times10^{-3}\text{mol/L}\times 2 \text{ mL}\times 2.8\times10^6 \text{ J/mol}}{1000 \text{ mL/L}} = 34.2 \text{ J}$$

Total converted chemical energy.

The final COD value of the electrolyte was 130 mg/L. This gives a COD removal efficiency of:

$$\frac{1170 \text{ mg COD/L} - 130 \text{ mg COD/L}}{1170 \text{ mg COD/L}} = 89\%$$

This means that 89% of the total chemical energy input (34.2×89%=30.4 J) was oxidized and assimilated and 11% (34.2-30.4=3.8 J) was retained in the electrolyte as residual COD.

Total chemical energy used for energy production.

The total charge passing through the external circuit, determined by integrating the generated current over time (Supplementary Fig. 8), was ~ 23.2 C.

The charge in 32 g of COD (equivalent to 1 mol of O_2) was $4\times9.65\times10^4$ C$=3.86\times10^5$ C. The total charge stored in the reduced electron acceptor was:

$$\frac{(1170 \text{ mg COD/L} - 130 \text{ mg COD/L})\times 2 \text{ mL} \times 3.86\times10^5 \text{ C}}{1000 \text{ mg/g}\times 1000 \text{ mL/L} \times 32 \text{ g COD}} = 25.1 \text{ C}$$

The above calculations indicate a coulombic efficiency of 23.2/25.1 x 100 = 92%: about 92% of the converted chemical energy (30.4×92%=28.1 J), or 89%×92%=82% of the initial chemical energy input, was used to meet microbial energy requirements. The remaining 100%-92%=8% of the converted chemical energy (30.4-28.1=2.3 J), or 89%-82%=7% of the initial chemical energy input, was used for microbial cell synthesis.

Distribution of generated energy.

The total electrical energy production was determined by integrating the power output over time (Supplementary Fig. 9), and was about 14.9 J. This represented 14.9/28.1=53% of the chemical energy used for energy production, 14.9/30.4=49% of the chemical energy converted, and 14.9/34.2=44% of the initial chemical energy input.

The theoretical oxidation potential of glucose is -0.43 V vs. SHE at pH 7, while the measured open circuit anode potential is -0.25 V vs. SHE. The 0.18 V overpotential is due to energy extraction by microorganisms for their own metabolism. The energy loss was

0.18 V×23.2 C=4.2 J. This is 4.2/28.1=15% of the chemical energy used for energy production, 4.2/30.4=14% of the chemical energy converted, and 4.2/34.2=12% of the initial chemical energy input.

Similarly, the theoretical reduction potential of Ag_2O/Ag is 0.76 vs. SHE at pH 7, while the measured open circuit cathode potential was 0.53 V vs. SHE. The 0.23 V activation potential results in an energy loss of 0.23 V×23.2 C=5.3 J. This is 5.3/28.1=19% of the chemical energy used for energy production, 5.3/30.4=18% of the chemical energy converted, and 5.3/34.2=16% of the initial chemical energy input.

Other energy losses (28.1-14.9-4.2-5.3=3.7 J) were due to internal resistance and diffusion issues. These losses were 100%-53%-15%-19%=13% of the chemical energy used for energy production, 92%-49%-14%-18%=11% of the chemical energy converted, and 82%-44%-12%-16%=10% of the initial chemical energy input.

Net electrical energy production

When using an electrochemical approach to regenerate the electrode, a voltage of 0.20-0.35 V was needed to regenerate the Ag_2O/Ag at a current of 0.01-1 mA/cm^2. With a coulombic efficiency of 97% (Supplementary Fig. 7), the electrical energy consumption is between 0.20 V×23.2 C/97%=4.8 J and 0.35 V×23.2 C/97%=8.4 J. This is between 4.8/30.4=16% and 8.4/30.4=28% of the chemical energy converted, and between 4.8/34.2=14% and 8.4/34.2=24% of the initial chemical energy input. Therefore, the net electrical energy production was between 14.9-8.4=6.5 J and 14.9-4.8=10.1 J, representing between 49%-28%=21% and 49%-16%=33% of the chemical energy converted, and between 44%-24%=20% and 44%-14%=30% of the initial chemical energy input.

Supplementary Figures and Legends

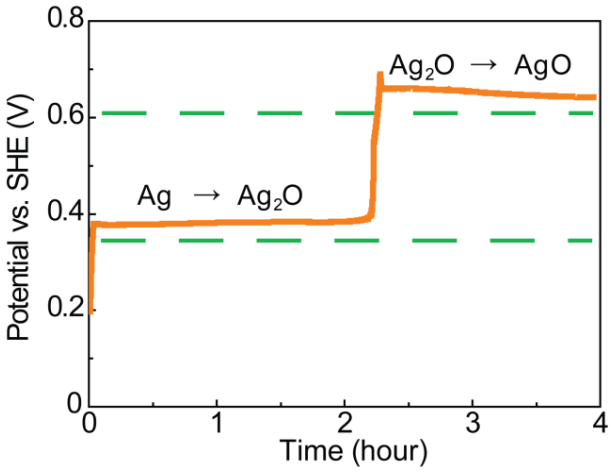

Supplementary Fig. 1. Potential profile of a carbon cloth supported silver electrode undergoing electrochemical oxidation in a sodium hydroxide (NaOH, 1M, pH 14) solution with a current density of 1 mA/cm^2. The dashed lines indicate the standard oxidation potential. To prepare a silver-oxide electrode, the oxidation process was stopped when the potential climbed to 0.3 V vs. Ag/AgCl (~0.5 V vs. SHE) to avoid formation of silver-peroxide (AgO).

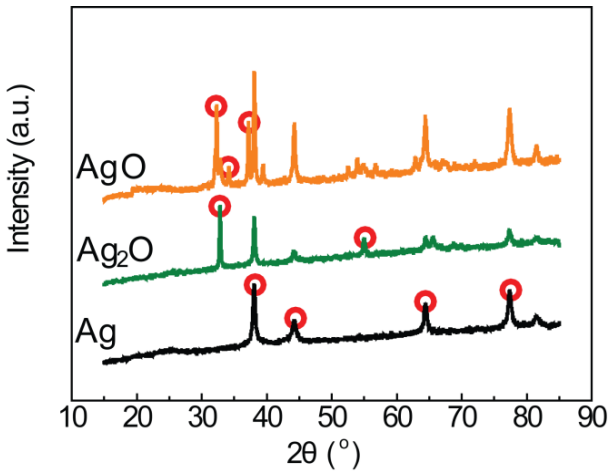

Supplementary Fig. 2. X-ray diffraction (XRD) patterns of silver (Ag), silver-oxide (Ag_2O), and silver-peroxide (AgO) on carbon cloth substrates. Characteristic peaks are circled in the figure.

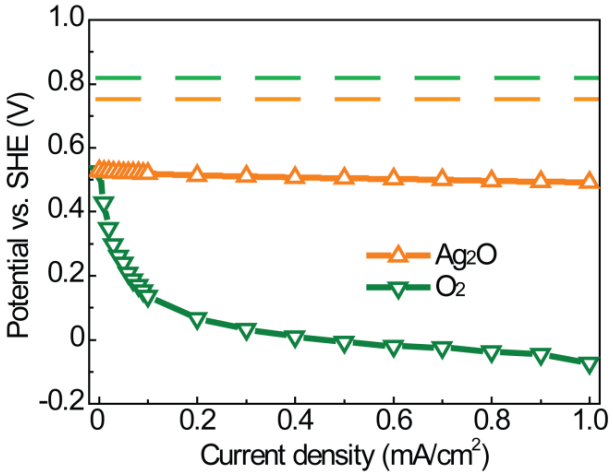

Supplementary Fig. 3. Polarization curves for silver-oxide reduction and oxygen reduction in a phosphate buffer solution (PBS, 200 mM, pH 7). Oxygen reduction was catalyzed by a commercially available platinum (Pt) electrode, and the electrolyte was bubbled with air (~100 mL/min) during measurement. The dashed lines indicate the standard reduction potentials (0.76 V for silver-oxide and 0.82 V for oxygen).

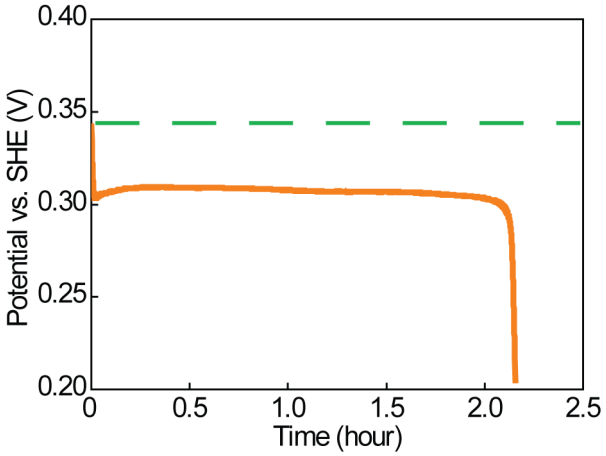

Supplementary Fig. 4. Potential profile of a Ag_2O/Ag electrode undergoing electrochemical reduction in a sodium hydroxide (NaOH, 1M, pH 14) solution with a current density of 1 mA/cm^2. The dashed lines indicate the standard reduction potential.

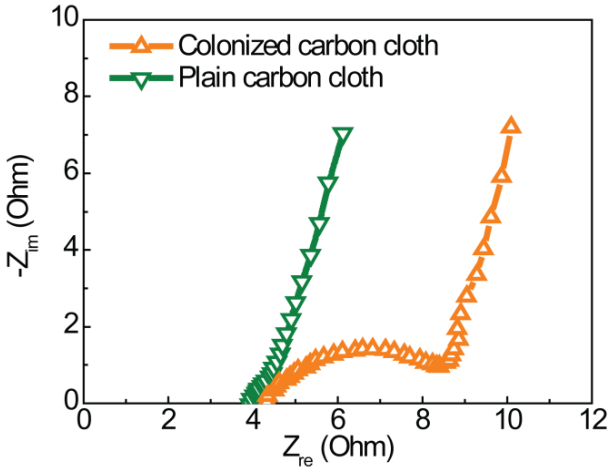

Supplementary Fig. 5. Nyquist curves of the electrochemical impedance spectroscopy test for a colonized carbon cloth electrode and a plain carbon cloth electrode in a glucose electrolyte (~1 g/L). The semicircle developed on the Nyquist curve of colonized carbon cloth electrode indicates charge transfer.

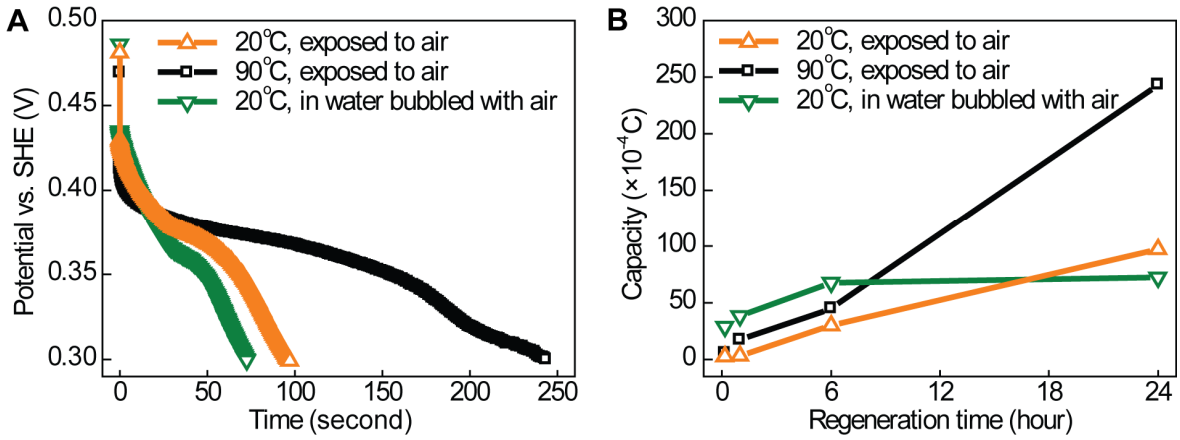

Supplementary Fig. 6. Direct re-oxidation of silver by oxygen. (A) Potential of Ag_2O/Ag electrode with a reducing current of 0.1 mA/cm^2 after 24-hours of regeneration. The electrolyte was a phosphate buffer solution (PBS, 200 mM, pH 7). (B) Oxidation capacity of the Ag_2O/Ag electrode after different regeneration times.

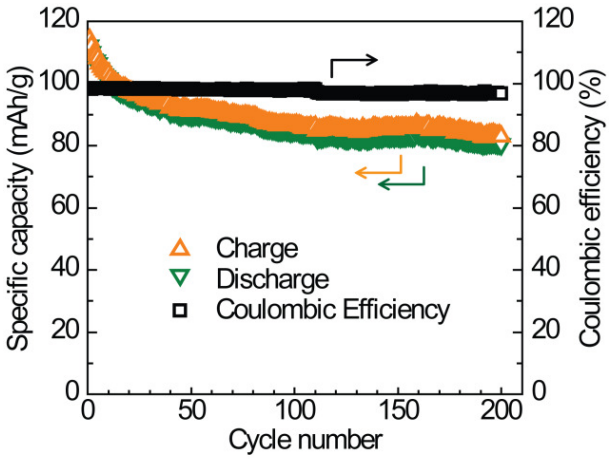

Supplementary Fig. 7. Cycling performance of a Ag_2O/Ag electrode in a NaOH (1M, pH 14) electrolyte with a current density of 1 mA/cm^2. Specific capacities are calculated based on the silver loading on the carbon cloth electrode. The coulombic efficiency was >97% over 200 cycles.

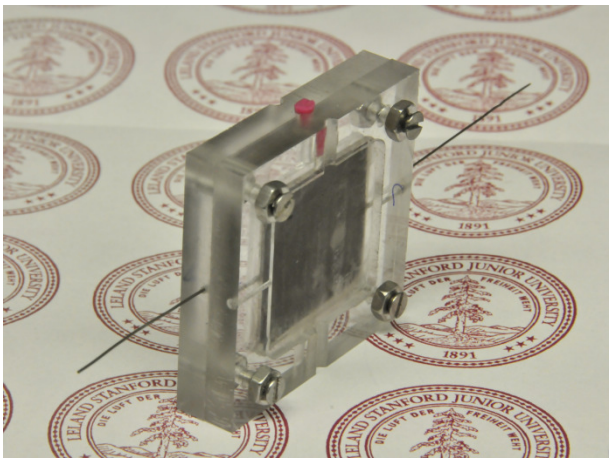

Supplementary Fig. 8. Plate-shaped MBs (3×3×0.3 cm^3) equipped with pre-colonized microbial anodes (3×3 cm^2) and silver-oxide cathodes (3×3 cm^2).

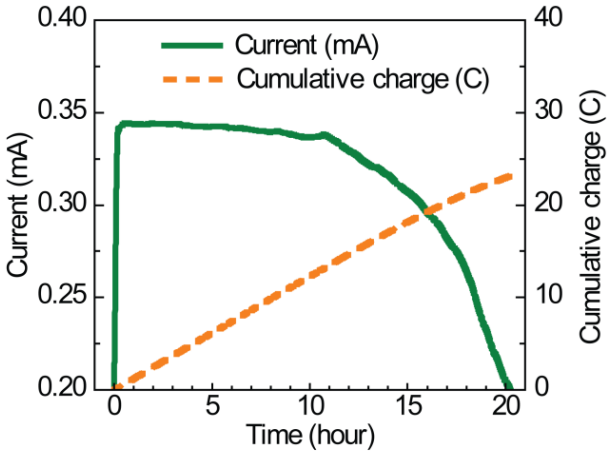

Supplementary Fig. 9. Current generation and cumulative charge of a plate-shaped MB with a 2000 Ω loading. The MB was equipped with a pre-colonized carbon cloth anode and a Ag_2O cathode. The electrolyte was a glucose solution (~1 g/L).

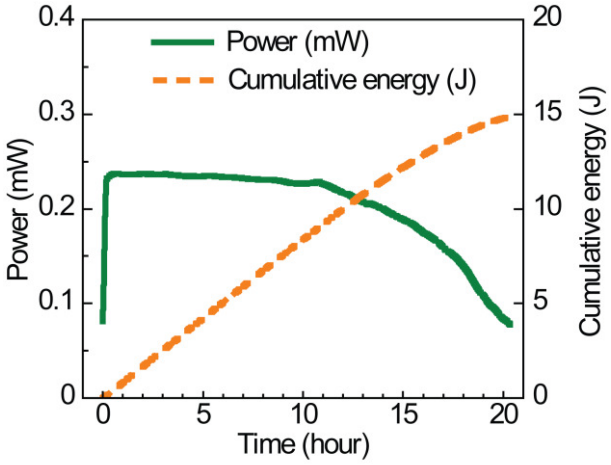

Supplementary Fig. 10. Power output and cumulative energy produced by a plate-shaped MB with a 2000 Ω loading. The MB was equipped with a pre-colonized carbon cloth anode and a Ag_2O cathode. The electrolyte was a glucose solution (~1 g/L).